The thin-film equation: recent advances and some new perspectives

2005 J. Phys.: Condens. Matter 17 S291

(http://iopscience.iop.org/0953-8984/17/9/002)

INSTITUTE OF PHYSICS PUBLISHING JOURNAL OF PHYSICS: CONDENSED MATTER

J. Phys.: Condens. Matter **17** (2005) S291–S307 doi:10.1088/0953-8984/17/9/002

The thin-film equation: recent advances and some new perspectives

Jürgen Becker and Günther Grün

Universität Bonn, Institut für Angewandte Mathematik, Beringstraße 6, 53115 Bonn, Germany

E-mail: becker@math.uni-bonn.de and gg@iam.uni-bonn.de

Received 24 November 2004
Published 18 February 2005
Online at stacks.iop.org/JPhysCM/17/S291

Abstract

This paper is concerned with mathematical aspects of lubrication equations. In the first part, we discuss recent analytical achievements for various types of thin-film equations. Of interest are issues like (non-)uniqueness, wetting behaviour and contact line motion, in particular optimal propagation rates and waiting time or dead core phenomena. In the second part, we shall present novel numerical results for thin-film flow on heterogeneous substrates based on entropy consistent schemes. Finally, we will be concerned with new algorithmic concepts for the simulation of thin-film flow of shear-thinning liquids.

(Some figures in this article are in colour only in the electronic version)

1. Introduction

This paper deals with mathematical aspects of the thin-film equation which enables a dimension-reduced description of the free-surface problem associated with Navier–Stokes equations in the case of laminar flow. The scope of this work is twofold. First, we shall survey the main contributions by mathematicians during the last six years—a period of major progress both in analysis and in numerics. In that way, we will draw a quite detailed picture of properties that solutions to these equations have. The features addressed include non-negativity results as well as dynamic issues (contact line propagation) or time-asymptotic results (characterization of stationary states). In the second part, we will present novel results on the numerical simulation both of thin-film flow on chemically patterned substrates and of non-Newtonian liquid flow on homogeneous substrates. Modelling aspects, however, are not in the centre of this paper. Indeed, a vast number of articles can be found in the literature which describe different facets of the long-wave approximation which is used to derive the thin-film equation from the free-surface problem related to the Navier–Stokes equation (see [41] and the references therein). Therefore, the starting point of this treatise will be the equation

$$\begin{aligned} &\eta u_t + \operatorname{div}(K(u)(\tau + \nabla\sigma)) - \operatorname{div}(m(u)\nabla p) = Q(u), \\ &p = -\sigma\Delta u + \phi'(u) \end{aligned} \tag{1}$$

0953-8984/05/090291+17$30.00

as derived by Oron *et al* [41]. Here, u denotes the time-dependent local thickness of a spreading liquid film on a plain surface, τ and σ stand for shear forces at the liquid–vapour interface and for surface tension, respectively, and η is the viscosity. The augmented Laplace pressure p is given as the sum of a linearized capillary term and the first variation of the effective interface potential ϕ.

The nonlinear mobility term $m(u)$ plays a crucial role for the qualitative behaviour of solutions. Its explicit form depends on the flow boundary condition at the liquid–solid interface. A no-slip condition entails

$$m(u) = \tfrac{1}{3}u^3,$$

whereas weighted slip conditions of the form

$$\vec{v}_{\mathrm{hor}}|_{z=0} = \beta^{3-n}u^{n-2}\frac{\partial \vec{v}_{\mathrm{hor}}}{\partial z}\bigg|_{z=0}$$

lead to

$$m(u) = \tfrac{1}{3}(u^3 + \beta^{3-n}u^n).$$

Here, $\beta \geqslant 0$ denotes the slip-length, $\vec{v}_{\mathrm{hor}}$ stands for the horizontal component of the velocity field, and z denotes the coordinate perpendicular to the substrate. Note that the choice $n = 2$ corresponds to the classical Navier slip condition. Similarly, the convective mobility $K(u)$ is a non-negative function that vanishes in zero. In the case of the Navier slip condition, it reads as $K(u) = \frac{1}{2}u^2 + \beta u$. Finally, the source term $Q(u)$ is to model effects of condensation or evaporation.

Let us give the outline of this paper. Section 2 is devoted to the free-boundary problem associated with equation (1) in the model situation of vanishing τ, Q, ϕ' and constant surface tension σ. Using a non-dimensionalized[1] version, we will hence consider the equation

$$\begin{aligned} &u_t + \mathrm{div}(m(u)\nabla\Delta u) = 0, \\ &u(\cdot, 0) = u_0(\cdot) \end{aligned} \tag{2}$$

which models the purely surface tension driven thin-film evolution. We will discuss necessary conditions on uniqueness of solutions and their implications on the design of numerical schemes. In section 3, we will be concerned with the no-slip paradoxon and with the relaxation of flow boundary conditions necessary to allow for droplet motion. In particular, various analytical results will be presented which provide the basic understanding of propagation rates for contact lines. In addition, questions of contact line retraction and of waiting time phenomena shall be addressed. Moreover, we will discuss some recent results on the behaviour of solutions to thin-film equations in shear-thinning rheologies. In this framework, the no-slip boundary condition is no longer incompatible with contact line motion. And in the final part of this section, we will be concerned with partial wetting and with effective interface potentials. Here, issues of film dewetting and droplet coarsening become important.

Having introduced concepts both to model molecular interaction and shear-thinning rheologies, the subsequent section will be about some new numerical results. Our first topic will be the formation of fluidic patterns induced by the underlying substrate structure. Numerical simulations will be presented which are based on convergent, entropy consistent and non-negativity preserving finite-element schemes. Moreover, we will cite corresponding non-negativity and stability results from the PhD thesis of the first author. It is worth mentioning that our results do not require pre-wetted substrates.

[1] Choosing a characteristic film thickness h_0 and a characteristic length scale l_0, equation (2) holds for the dimensionless variables $\hat{u} = u/h_0$, $\hat{x} = x/l_0$ and $\hat{t} = \frac{h_0^3\sigma}{\eta l_0^4}t$.

Finally, we will address the numerical simulation of non-Newtonian flow. We suggest a new numerical scheme for thin-film flow in shear-thinning rheologies that is inspired by our concept of admissible entropy–mobility pairs recently developed for the case of Newtonian rheology (see [31, 32, 30]). Numerical results will indicate that a subtle splitting of the non-linear operator ensures non-negativity of discrete solutions and permits us to capture the contact line propagation rate precisely as it was identified analytically in [1]. For the aspects of numerical analysis, we refer to the forthcoming paper [4].

Notation. In this paper, we identify the physical substrate mathematically with a domain Ω in $\mathbb{R}^N$, $N \in \{1, 2\}$. In particular, the letter N will always be used to denote the spatial dimension. Assuming that u models the film thickness, the wetted area at time t is given as the set $[u(\cdot, t) > 0] := \{x \in \Omega : u(x, t) > 0\}$. At time t, the contact line between the liquid, solid, and vapour phases is defined as $\partial[u(\cdot, t) > 0]$. Similarly, the support of u at time t is given by $\operatorname{supp}(u(\cdot, t)) := [u(\cdot, t) > 0] \cup \partial[u(\cdot, t) > 0]$. We use the N-dimensional Lebesgue measure $\mathcal{L}^N$ to measure the area of subdomains of the substrate. By Ω_T, we denote the space–time cylinder $\Omega \times (0, T)$. Sometimes, we will use the abbreviations u_t and u_x for $\frac{\partial}{\partial t}u$ and $\frac{\partial}{\partial x}u$, respectively. Let us give some basic notions of function spaces. For non-negative integers α, β, the set of continuous functions which are differentiable α times with respect to space and β times with respect to time are denoted by $C^{\alpha,\beta}(\Omega_T)$. For $\gamma, \sigma \in (0, 1)$, $C^{\gamma,\sigma}(\Omega_T)$ stands for the space of continuous functions which are Hölder continuous with respect to space and time with Hölder exponents γ and σ, respectively. Slightly more advanced is the notion of $L^p(0, T; X)$. Here X is a function space itself, and $L^p(0, T; X)$ is—loosely speaking—the set of mappings $x : (0, T) \to X$ such that $\|x(\cdot)\|_X$ is summable to the exponent $p \geqslant 1$. Finally, we use $(x)_+$ as an abbreviation for $\max\{x, 0\}$.

2. The free boundary problem and questions of uniqueness

Under the assumption that solutions $u(x, t)$ to equation (1) are zero at a time t for sets of positive spatial Lebesgue measure, i.e. $\mathcal{L}^N([u(x, t) = 0]) > 0$, equation (1) implicitly defines a free boundary problem, with the free boundary given by the boundary of the set $[u(\cdot, t) > 0]$. Translated into physical terms, the free boundary is nothing else than the contact line connecting liquid, solid, and vapour phase. In the seminal paper [9], Bernis and Friedman considered for positive n the equation

$$\begin{aligned} &u_t + (u^n u_{xxx})_x = 0, \\ &u(\cdot, 0) = u_0(\cdot) \end{aligned} \tag{3}$$

on space–time cylinders $\Omega_T := (-a, a) \times (0, T)$. For the case of mass-conserving boundary conditions, they introduced the following solution concept, paying tribute to the fact that at the contact line solutions cannot be four times differentiable with respect to spatial coordinates.

Definition 2.1. *Let $\Omega = (-a, a)$ be a bounded interval. A non-negative function $u \in C^{4,1}([u > 0]) \cap C^{1/2,1/8}(\Omega_T)$ satisfying $u^{\frac{n}{2}}u_{xxx} \in L^2([u > 0])$ and $\frac{\partial}{\partial x}u = \frac{\partial^3}{\partial x^3}u = 0$ in $\partial\Omega$ is called a weak solution to equation (3), if*

$$\int_0^\infty \int_\Omega (u - u_0)\zeta_t + \int_0^\infty \int_{[u(\cdot,t)>0]} u^n u_{xxx}\zeta_x = 0 \tag{4}$$

for arbitrary $\zeta \in C^1(\mathbb{R}^+ \times \bar{\Omega})$ satisfying $\zeta(\cdot, T) = 0$.

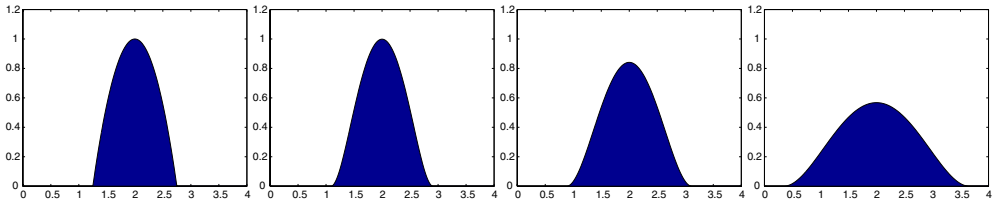

Figure 1. Simulation to the equation $u_t + \partial_x(u^2 u_{xxx}) = 0$; the snapshots show times $t = 0$, 0.001, 0.01, 0.1.

Remark. Formally, the weak formulation (4) is obtained from (3) by multiplication by ζ and integration by parts with respect to time and space, respectively. Note that in such a way the requirements on the differentiability of solutions can be weakened.

Obviously, the function $u(x,t) = M(b^2 - x^2)_+$ is a stationary weak solution provided $\pm b \in \Omega$ and M is a positive real number. On the other hand, the solution sketched in figure 1 is a non-stationary weak solution having the same initial data. In particular, it can be proven that this solution satisfies (4), too. Hence, for given initial data uniqueness cannot be guaranteed. The reason for such an ambiguity is the following. On the one hand we are implicitly dealing with a free boundary problem for a fourth order equation, but on the other hand in definition 2.1 we specify instead of three conditions at the free boundary only two of them, namely the natural ones

$$u|_{\partial[u(\cdot,t)>0]} = u^n u_{xxx}|_{\partial[u(\cdot,t)>0]} = 0.$$

Therefore, we cannot expect uniqueness without changing the solution concept accordingly.

One remedy could be to prescribe the contact angle at the contact line. Besides the one-dimensional approach of Otto [42] who studies the lubrication equation related to Darcy flow in a Hele–Shaw cell and who proves the existence of solutions with constant non-zero contact angle, rigorous mathematical results so far were only available for zero-contact-angle solutions.

Technically, these are distinguished due to the fact that a zero-contact-angle can be enforced implicitly via integral estimates. And since it is still an open problem how to formulate the free boundary problem explicitly, the implicit approach using the partial differential equation globally still serves as the silver bullet for the analytical understanding. So let us introduce these integral estimates.

With regard to non-negativity and regularity at the contact line, the so called α-entropy estimate [13, 18, 6, 12] is essential. In the case of the model problem[2]

$$\begin{aligned} &u_t + \operatorname{div}(u^n \nabla \Delta u) = 0 && \text{in } \Omega \times (0,T), \\ &u(\cdot,0) = u_0 && \text{on } \Omega, \end{aligned} \tag{5}$$

it can be established for $\alpha \in (\max\{-1, \frac{1}{2} - n\}, 2 - n) \setminus \{0\}$ in the following form:

$$\frac{1}{\alpha(\alpha+1)} \int_\Omega u^{\alpha+1}(\cdot,T) + C^{-1} \int_0^T \int_\Omega (|\nabla u^{\frac{\alpha+n+1}{4}}|^4 + |D^2 u^{\frac{\alpha+n+1}{2}}|^2) \leqslant \frac{1}{\alpha(\alpha+1)} \int_\Omega u_0^{\alpha+1}. \tag{6}$$

There is no direct physical interpretation of this estimate—despite its importance it is of a merely technical nature.

[2] If $\Omega \neq \mathbb{R}^N$, boundary conditions are necessary. A possible choice is mass-conserving boundary conditions $\frac{\partial}{\partial \nu} u = u^n \frac{\partial}{\partial \nu} \Delta u = 0$ on $\partial\Omega \times (0,T)$. We will not further dwell upon this point as it is irrelevant for the local behaviour near the contact line.

This is in strong contrast to the second integral estimate given by

$$\tfrac{1}{2}\int_\Omega |\nabla u(\cdot,T)|^2 + \int_0^T \int_\Omega u^n |\nabla \Delta u|^2 = \tfrac{1}{2}\int_\Omega |\nabla u_0|^2 \tag{7}$$

which is called the energy estimate. Indeed, the first term on the left-hand side is just the linearized capillary energy in the complete wetting regime. Similarly, the second term on the left-hand side describes the energy dissipated due to viscous friction. Note that both the stationary and the non-stationary solution to initial data $u_0(x) = M(b^2 - x^2)_+$ satisfy (7). In contrast, only the non-stationary (zero-contact-angle) solution obeys (6). For this reason, such a solution is called an *entropy solution* or a *strong solution*. Finally, let us emphasize the relevance of these observations for the design of numerical schemes. Given a numerical scheme which does not satisfy additional estimates besides the energy estimate (7), the solution in the continuous setting is not unique and therefore no convergence results can be formulated in the case of the free boundary problem. In contrast, for the entropy schemes developed in [31, 30], convergence of subsequences towards entropy solutions is proven. Moreover, assuming the uniqueness of entropy solutions, the whole sequence of discrete solutions has to converge towards the entropy solution.

3. Droplet propagation: spreading versus no-slip-paradoxon

3.1. Basic observations

A closer look at the equation (5) reveals its invariance under the scalings

$$x = k\hat{x}, \qquad t = k^\gamma \hat{t}, \qquad u = k^{-N}\hat{u}$$

with $\gamma = 4 + nN$, N the space dimension. Hence, the existence of compactly supported self-similar solutions of the form

$$u(x,t) = t^{-\frac{N}{4+nN}} U\left(\frac{x}{t^{\frac{1}{4+nN}}}\right) \tag{8}$$

would be expected for arbitrary $n > 0$. Surprisingly, such solutions only exist if $n \in (0, 3)$ as proven in space dimension $N = 1$ in [10] and for the higher-dimensional case in [23].

Moreover, in space dimension $N = 1$ Beretta *et al* [6] proved that for $n > 4$ contact lines are constant in time. A related result, which states that for $n \in [3, 4)$ solutions with constant support (= time-independent wetted area) can be constructed for arbitrary initial configurations, was recently proposed by Winkler [45].

Altogether, this reveals $n = 3$ to be a borderline value for this equation. In particular, it is in good agreement with the classical observation made by Dussan and Davis [22] that in the case of a no-slip boundary condition droplet motion in Newtonian rheologies is only possible at the expense of infinite energy dissipation at the moving contact line. During the last decade, many ansätze were proposed to relax the dissipation singularity. A common starting point is the formula

$$\vec{v}_{\mathrm{hor}}|_{z=0} = \beta^{3-n} u^{n-2} \frac{\partial \vec{v}_{\mathrm{hor}}}{\partial z}\bigg|_{z=0} \tag{9}$$

fixing the flow condition at the liquid–solid interface.

In general, n may vary between zero and three; distinguished, however, is the case $n = 2$ which corresponds to the classical Navier-slip condition (see [37], and [35] for its relevance with respect to flow over rough surfaces). Also smaller values of n have been suggested in the physical literature (see [25, 26, 38]) to formulate phenomenological models for precursor films.

From the mathematical point of view, these approaches entail a modified thin-film equation given by

$$\begin{aligned} &u_t + \operatorname{div}((u^3 + \beta^{3-n}u^n)\nabla\Delta u) = 0, \\ &u(\cdot, 0) = u_0(\cdot) \end{aligned} \tag{10}$$

for parameters $n \in (0, 3)$.

Following the results of Dal Passo *et al* [18], it is solely the regularity of the function $m(x) = x^3 + \beta^{3-n}x^n$ near its zero point $x_0 = 0$ that determines the qualitative behaviour of solutions. This applies to questions of spreading or non-spreading as well as to questions of locally preserved positivity and local film rupture.

As a consequence, the model problem (5) with $n \in (0, 3)$ attracted a lot of interest from analysts. With respect to timescales of contact line propagation, however, the picture becomes biased as equation (10) exhibits fewer scaling invariances than equation (5). For this reason, self-similar solutions to equation (10) do not exist.

3.2. Scaling laws

In this section, we intend to review some recent results on contact line motion—both for equation (10) in one space dimension and for equation (5) in arbitrary dimensions $N \leqslant 3$. Apparently, self-similar solutions set the scale; nevertheless, many additional effects can be observed in case of arbitrary non-negative initial data. In general, the results to be presented below pertain to entropy solutions (i.e. zero-contact-angle solutions satisfying estimate (6)).

Let us begin this exposition with the following statement which summarizes results of [7, 8, 33] for space dimension $N = 1$ and of [13, 29, 28] for the multi-dimensional case.

Theorem 3.1. *Let u be an entropy solution to equation (5) on the space–time-cylinder $\mathbb{R}^n \times (0, T)$ to continuous, non-negative initial data u_0 such that* $\operatorname{supp}(u_0) \subset B(0, R_0)$. *Then a positive constant $C = C(n, N, \|u_0\|_{L^1(\mathbb{R}^N)})$ exists such that*

$$\operatorname{supp}(u(\cdot, t)) \subset B(0, R(t)) \tag{11}$$

where

$$R(t) \leqslant R_0 + Ct^{\frac{1}{4+nN}}. \tag{12}$$

Note that the time-exponent in (12) is identical to the parameter $\gamma = \frac{1}{4+nN}$ which characterizes contact line propagation for self-similar solutions.

Hence, the estimate (12) is asymptotically optimal. In this context the question arises of whether droplet profiles converge for large t towards the self-similar profile given by (8). So far, an affirmative answer to this question could only be given in space dimension $N = 1$ by Carrillo and Toscani [16]. For further results on finite speed of propagation, in particular on local properties if the initial support (= the initially wetted area) is not convex, we refer to [13, 27]. It is worth mentioning that the above mentioned result gives only an upper bound on the wetted area whereas information about backward propagation is missing. When investigating this topic, another facet of n-sensitivity becomes evident. It can be summarized within the following theorem.

Theorem 3.2. *Let u be a strong solution as considered in theorem 3.1. Then the following positivity results hold.*

(1) If u_0 is strictly positive on a subset $E \subset \operatorname{supp}(u_0)$ of positive measure, then we have for all $t > 0$ that $\int_E u(x, t)\,\mathrm{d}x > 0$ provided $n > \frac{3}{2}$.

Figure 2. Dead core phenomenon: the snapshots show a solution to the equation $u_t + \partial_x (u u_{xxx}) = 0$ on the interval $[0, 1]$. The first picture shows the initial data, $u_0(x) = (x - 0.5)^4 + 0.001$; the subsequent ones the solution at times $t = 0.002$, 0.012 and 0.040. Although initial data are strictly positive, the solution does not stay strictly positive at all times.

(2) If $N = 2$ and $n > 3$ or if $N = 1$ and $n \geqslant 2$, then $u_0(x) > 0$ implies $u(x, t) > 0$ for almost all $t \in (0, T)$.

Remark.

(1) The first assertion shows in particular that backward motion of contact lines cannot happen as soon as $n > \frac{3}{2}$.
(2) Numerical experiments (see figure 2) indicate that for $n \leqslant \frac{3}{2}$ finite-time rupture can occur.
(3) For $t \to \infty$, however, it can be proven that all solutions spread, independently of $n \in (0, 3)$. For more details, see the decay estimates presented in [13].

Observing that for values of $n \in (0, \frac{3}{2})$ backward motion of contact lines takes place, the question arises of for which initial data the onset of forward motion is delayed. To put it differently—can we formulate a condition on the initial droplet profile which guarantees that for some positive time T^* the wetted area does not increase? Such a phenomenon is called a waiting time phenomenon, and the following theorem summarizes results of [19, 27].

Theorem 3.3. *Let $N \in \{1, 2, 3\}$ and $n \in (0, 3)$. Let u be an entropy solution to compactly supported, non-negative initial data. Assume that x_0 is a boundary point of* $\mathrm{supp}(u_0)$ *such that*

(i) there is a cone $\mathcal{C}(x_0, 2\theta) \subset \mathbb{R}^N$ with vertex x_0 and opening angle 2θ such that $\mathrm{supp}(u_0) \cap \mathcal{C}(x_0, 2\theta) = \emptyset$,
(ii) near x_0 initial data are sufficiently regular; more precisely, there is a constant $C > 0$ such that $|\nabla u_0(x)| \leqslant C|x - x_0|^{\frac{4}{n}-1}$ for x near x_0.

Then a waiting time phenomenon occurs in the sense that a positive time T^* exists such that $\mathcal{C}(x_0, \theta) \cap \mathrm{supp}(u(\cdot, t)) = \emptyset$ for all $t \in (0, T^*)$.

Remark. According to theorem 3.3, a waiting time phenomenon can be observed if $n \in [3/2, 3)$, too. Therefore we may infer from theorem 3.2 that in this case the contact line locally does not move during the time-interval $(0, T^*)$.

At the end of this section it remains to discuss how a mobility $m(u) = u^3 + \beta^{3-n} u^n$ changes the propagation rate. Obviously, in comparison with (5), equation (10) loses one of its scaling invariances. For this reason, self-similar solutions are no longer expected to exist—and in fact, they do not exist.

As it has already been conjectured in the physics community (see [20]) and as it recently could be proven mathematically in a rigorous way for the one-dimensional case by Giacomelli and Otto [24], on intermediate timescales the spreading rate $t^{\frac{1}{4+n}} = t^{\frac{1}{7}}$—which is formally expected in the no-slip case—is corrected only logarithmically. For large t however, as soon as the film becomes sufficiently flat, the $\beta^{3-n} u^n$-term starts to dominate and therefore the asymptotic propagation rate is that of the model equation (5) as formulated in theorem 3.1.

3.3. Non-Newtonian rheologies—shear-thinning liquids

Another approach to overcome the no-slip paradoxon mentioned above is to consider instead of Newtonian rheologies shear-thinning constitutive laws. This approach is particularly well suited to model the flow behaviour of polymer melts (see [15]). Let us describe two mechanisms proposed in the physical literature. Assuming a viscosity–shear relation like

$$\mu = \mu_0 |\tau|^{\alpha-1} \tag{13}$$

for numbers $\alpha \in (0, 1)$, μ the viscosity, τ the shear stress, together with a no-slip-flow condition at the liquid–solid interface, the thin-film equation

$$u_t + \frac{\alpha}{2\alpha+1} \operatorname{div}\left(u^{\frac{2\alpha+1}{\alpha}} |\nabla \Delta u|^{\frac{1-\alpha}{\alpha}} \nabla \Delta u\right) = 0 \tag{14}$$

is derived as a model equation.

A closer look at (13) reveals that the viscosity μ tends to infinity for $\tau \to 0$. To exclude singular behaviour of that kind, Weidner and Schwartz [44] proposed

$$\frac{1}{\mu} = \frac{1}{\mu_0}\left(1 + \left|\frac{\tau}{\tilde{\tau}}\right|^{\frac{1-\alpha}{\alpha}}\right), \qquad \alpha \in (0, 1) \tag{15}$$

as the constitutive relation between viscosity and shear stress. Here, μ_0 is the viscosity at zero shear stress and $\tilde{\tau}$ denotes the shear stress at which viscosity attains the value $\frac{1}{2}\mu_0$.

A lubrication approximation leads to

$$u_t + \operatorname{div}\left(u^3\left(1 + |u \nabla \Delta u|^{\frac{1-\alpha}{\alpha}}\right) \nabla \Delta u\right) = 0 \tag{16}$$

in the non-dimensionalized case.

For $\alpha \in (0, 1)$ both the equations (14) and (16) allow for travelling wave solutions (see [36, 14])—and as proven by Aronson *et al* in [2] equation (14) has source-type solutions both with finite and with zero contact angle. Those with zero contact angle could be proven to be unique. Moreover, by scaling analysis the propagation rate was determined to be given by $t^{\frac{\alpha}{5+2\alpha}}$, $\alpha \in (0, 1)$. In contrast, equation (16) does not allow for self-similar solutions—again due to a lack of scaling invariances. In a very recent paper, Ansini and Giacomelli [1] studied in one space dimension questions of existence and propagation rates for zero-contact-angle solutions to (14). Based on a combination of the energy estimate and the techniques developed in [19], it was not only possible to recapture the exponent $\beta = \frac{\alpha}{5+2\alpha}$ as the asymptotic spreading exponent. Furthermore, the number $\gamma = \frac{1+3\alpha}{3\alpha}$ was identified as the characteristic exponent for a waiting time phenomenon to occur. More precisely, the following result holds.

Theorem 3.4. *Let u be a solution of equation (14) to compactly supported, non-negative initial data and assume the spatial dimension $N = 1$. Assume that x_0 is a boundary point of* $\operatorname{supp}(u_0)$ *such that $|\frac{\partial}{\partial x} u_0(x)| \leqslant C|x - x_0|^{\gamma-1}$ for $|x - x_0|$ sufficiently small. Then a waiting time phenomenon occurs.*

3.4. Interface potentials and partial wetting

In the previous chapters the case of solely surface tension driven thin-film flow has been considered. However, in many applications additional forces like gravity and van der Waals interactions play a significant role. These forces enter the evolution equation

$$u_t - \operatorname{div}(m(u) \nabla p) = 0 \tag{17}$$

via the effective interface potential ϕ which is part of the augmented Laplace pressure

$$p = -\Delta u + \phi'(u). \tag{18}$$

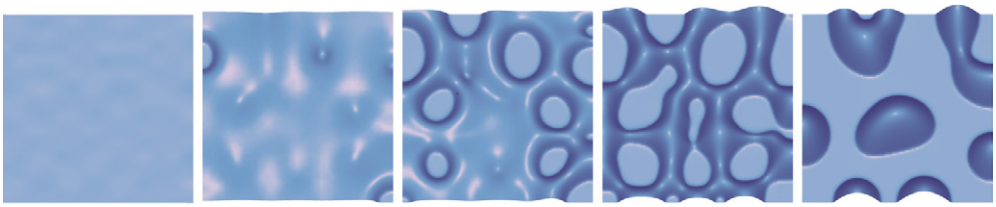

Figure 3. Numerical simulation of dewetting polymer film: the pictures show a square of side length 1.5 μm at times $t = 218$, 3177, 3445, 3805, and 5245 s. Initially, the film is 3.9 nm thick and slightly perturbed. The simulation used the interface potential $\phi = -\frac{A}{12\pi}u^{-2} + \varepsilon u^{-8}$ and the following experimentally determined parameters [5]: surface tension 0.0308 N m^{-1}, viscosity 12 000 Pa s, Hamaker constant $A = 2.2 \times 10^{-20}$ J, and $\varepsilon = 6.25 \times 10^{-76}$ J m^6.

Disjoining and conjoining intermolecular forces due to van der Waals interactions and Born repulsion are usually modelled by potentials of the form

$$\phi(u) = -a_1 u^{-l_1} + a_2 u^{-l_2}. \tag{19}$$

The standard 6–12 Lennard-Jones pair potential corresponds to $l_1 = 2$, $l_2 = 8$ in this model [34]. Here, the u^{-2} term models long-range attractive forces, whereas the second term models the short-range stabilizing effect of Born repulsion.

In one space dimension, problem (17)–(19) is well posed and the existence of a Hölder-continuous weak solution u is proven if $l_2 > \max\{l_1, 2\}$ [32]. Moreover, this solution is strictly positive if initial data are strictly positive.

These results allow us to define an energy

$$\mathcal{E} = \int_\Omega \tfrac{1}{2}|\nabla u|^2 + \phi(u)\,\mathrm{d}x, \tag{20}$$

which is monotonically decreasing, with the rate of dissipation given by

$$\frac{\mathrm{d}\mathcal{E}}{\mathrm{d}t} = -\int_\Omega m(u)|\nabla p|^2 \leqslant 0. \tag{21}$$

In [11], Bertozzi *et al* proved the existence of a global minimizer of $\mathcal{E}$ for space dimension $N = 1$. Moreover, it is shown by bifurcation analysis that multi-droplet configurations are only metastable and that for $t \to \infty$ the film profile converges to a one-droplet configuration.

In higher space dimensions, pointwise strict positivity can no longer be guaranteed. Nevertheless, for the entropy consistent finite-element schemes developed in [30], convergence of discrete solutions to entropy solutions in appropriate function spaces could be proven. This finite-element scheme has been applied to simulate the flow of thin polymer films on silicon wafers [5, 39, 40], and the results of the simulations have been found to match the experimental results both qualitatively and quantitatively.

Figure 3 shows a very typical example for the dewetting of thin polymer films. Initially, the film is almost flat and covers the surface. After some time, first holes appear, these holes coalesce and in the end only droplets remain. This multiple-droplet situation is still unstable: The larger droplets continue to grow at the expense of the smaller ones, until for larger times only one droplet is expected to persist. But this coarsening process happens on a different timescale than the dewetting process. As simulations in $N = 1$ show, the coarsening process is several orders of magnitude slower than the dewetting process [11]. Therefore, due to numerical costs, only the beginning of this process is visible in 2D simulations.

4. Numerical approaches

4.1. Newtonian liquid films on homogeneous substrates

In this section we present in detail the algorithm used for the simulations shown in figures 1–3. The algorithm computes a discrete solution of the problem

$$\begin{aligned} u_t - \operatorname{div}(m(u)\nabla p) &= 0 \qquad \text{on } \Omega \times (0,T) \\ p &= -\Delta u + \phi'(u) \qquad \text{on } \Omega \times (0,T) \end{aligned} \tag{22}$$

subjected to no-flux boundary conditions

$$\frac{\partial u}{\partial \nu} = \frac{\partial p}{\partial \nu} = 0 \qquad \text{on } \partial\Omega \times (0,T) \tag{23}$$

and initial data

$$u(\cdot,0) = u_0(\cdot) \qquad \text{on } \Omega. \tag{24}$$

We assume that the mobility m is given by $m(s) = (s)_+^n$, $n \in (0,\infty)$. We furthermore assume that the effective interface potential $\phi(u)$ is bounded from below and that it is given as the sum of a convex function $\phi_+(u) \in C^1(\mathbb{R})$ and a concave function $\phi_-(u) \in C^1(\mathbb{R})$.

So let $\mathcal{T}_h$ be a regular and admissible triangulation of the domain $\Omega \subset \mathbb{R}^N$, $N = 1, 2$ with simplicial elements (see Ciarlet's monograph [17]). If $N = 2$, we suppose in addition that the triangulation is *rectangular* in the sense that each triangle $T \in \mathcal{T}_h$ is a rectangular one. This induces a slight restriction on the class of domains for which our method works. In the following we implicitly assume that Ω permits triangulations $\mathcal{T}_h$ having this property.

By V^{h}, we denote the space of continuous functions which are linear on each element $E \in \mathcal{T}_h$. In the following, elements of V^{h} will be denoted by capitals; functions contained in nondiscrete function spaces will be denoted by lower-case characters. A function $V \in V^{\mathrm{h}}$ is uniquely defined by its values on the set of nodes $\mathcal{N}_h = \{x_j\}_{j=1}^{\dim V^{\mathrm{h}}}$ of the triangulation $\mathcal{T}_h$. A set of basis functions dual to the set of nodal points $\mathcal{N}_h$ is given by the 'hat'-type functions $\varphi_j \in V^{\mathrm{h}}$ with $\varphi_j(x_i) = \delta_{ij}$. Furthermore, we introduce the lumped mass scalar product given as

$$(\Theta, \Psi)_h := \int_\Omega \mathcal{I}_h(\Theta\Psi), \tag{25}$$

where $\mathcal{I}_h : C^0(\Omega) \to V^{\mathrm{h}}$ is the interpolation operator defined by $\mathcal{I}_h u = \sum_{j=1}^{\dim V^{\mathrm{h}}} u(x_j)\varphi_j$. The lumped mass scalar product is an approximation of order h of the usual L^2-scalar product on Ω, which will be denoted by $(\cdot,\cdot)$.

Let the time interval $I := [0,T]$ be subdivided in intervals $(t_k, t_{k+1}]$ with $t_{k+1} = t_k + \tau_k$ for time increments $\tau_k > 0$ and $k = 0, \ldots, K-1$. Then an implicit, backward Euler scheme for equations (17) and (18) reads as follows.

Given $U^0 = \mathcal{I}_h u_0 \in V^{\mathrm{h}}$, find functions $U^{k+1} \in V^{\mathrm{h}}$ and $P^{k+1} \in V^{\mathrm{h}}$, $k = 0, \ldots, K-1$ such that

$$\left(U^{k+1} - U^k, \Theta\right)_h + \tau_k \left(M_\sigma(U^{k+1})\nabla P^{k+1}, \nabla\Theta\right) = 0, \tag{26}$$

$$\left(\nabla U^{k+1}, \nabla\Psi\right) + \left(\phi_+'(U^{k+1}), \Psi\right)_h + \left(\phi_-'(U^k), \Psi\right)_h = \left(P^{k+1}, \Psi\right)_h \tag{27}$$

for all $\Theta, \Psi \in V^{\mathrm{h}}$.

Note that the destabilizing term ϕ_-' is discretized explicitly in time, whereas the stabilizing term ϕ_+' is dicretized implicitly in time. This distinction is essential to bound the free energy at time T by the free energy of the initial data.

To make discrete versions of the entropy estimate available, we apply the concept of admissible entropy mobility pairs introduced in [31] to define a discrete mobility M_σ.

We call a pair of functions $G_\sigma : \mathbb{R} \to \mathbb{R}_0^+$, $M_\sigma : V^h \to \bigotimes_{k=1}^{|\mathcal{T}_h|} \mathbb{R}^{N\times N}$ an *admissible entropy–mobility pair with respect to the triangulation* $\mathcal{T}_h$ if the following axioms are satisfied:

(i) $M_\sigma : V^h \to \bigotimes_{k=1}^{|\mathcal{T}_h|} \mathbb{R}^{N\times N}$ is continuous,
(ii) $M_\sigma(U)|_E = m_\sigma(U)\mathrm{Id}$ if $U|_E$ is constant,
(iii) $M_\sigma(U)\nabla \mathcal{I}_h G'_\sigma(U) = \nabla U$, where $G_\sigma(s) := \int_A^s g_\sigma(r)\,\mathrm{d}r$ with $g_\sigma(s) = \int_A^s m_\sigma(r)^{-1}\,\mathrm{d}r$,
(iv) on each element E, the matrix $M_\sigma(U)|_E$ is symmetric and positive semidefinite.

This means that given a function $U \in V^h$, we find an associated field of $N \times N$ matrices which are constant on each element of the triangulation. By construction, G_σ is non-negative and convex. Here, m_σ is an appropriate approximation for the continuous mobility m. In the case $n \geqslant 1$, we take for instance $m_\sigma(u) := m(\max(\sigma, u))$ with a positive parameter $\sigma \ll 1$. In the case $0 < n < 1$, a different approach has to be applied—for details we refer to [31].

To calculate the $N \times N$ matrix M_σ on an element $E \in \mathcal{T}_h$ we proceed as follows. If $N = 1$, E is just an interval bounded by two adjacent nodal points: $E = [x_i, x_{i+1}]$. A discrete mobility satisfying the axioms above can be defined by

$$M_\sigma(U)|_{[x_i,x_{i+1}]} = \varrho(U(x_i), U(x_{i+1})) \tag{28}$$

where ϱ is given by

$$\varrho(x, y) := \begin{cases} \left(\dfrac{1}{y-x}\displaystyle\int_x^y \frac{\mathrm{d}s}{m_\sigma(s)}\right)^{-1} & \text{if } x \neq y \\ m_\sigma(x) & \text{if } x = y. \end{cases} \tag{29}$$

If $N = 2$, $\mathcal{T}_h$ consists of rectangular triangles. Each triangle $E \in \mathcal{T}_h$ can be mapped onto a reference triangle $\hat{E}$ with nodes at 0, $\alpha_1 e_1$ and $\alpha_2 e_2$, by an affine transformation $x \mapsto \hat{x} = x_0 + A^{-1}x$, where A is an orthogonal matrix. Here, (e_1, e_2) denotes the canonical basis of $\mathbb{R}^2$. On such a reference triangle $\hat{E}$ the axioms above are satisfied by the 2×2 matrix

$$\hat{M} = (\delta_{ij}\varrho(U(0), U(\alpha_i e_i)))_{i,j=1,2}. \tag{30}$$

Now the mobility matrix on E is given by $M := A\hat{M}A^{-1}$.

To solve (26) and (27), we recall that a function $U \in V^h$ is uniquely defined by its values on $\mathcal{N}_h$. For notational simplicity, we will not distinguish between $U \in V^h$ and the coordinate vector of U with respect to the canonical basis $\varphi_i, i = 1, \ldots, \dim(V^h)$. So we define the matrices M_h, L_h and $L_h^M(U)$ by

$$M_h := \left((\varphi_i, \varphi_j)_h\right)_{i,j=1}^{\dim V^h}, \tag{31}$$

$$L_h := \left((\nabla\varphi_i, \nabla\varphi_j)\right)_{i,j=1}^{\dim V^h}, \tag{32}$$

$$L_h^M(U) := \left((M_\sigma(U)\nabla\varphi_i, \nabla\varphi_j)\right)_{i,j=1}^{\dim V^h}, \tag{33}$$

and see that we have to find in each timestep a solution U^{k+1} of the equation

$$U^{k+1} - U^k + \tau_k M_h^{-1} L_h^M(U^{k+1})[M_h^{-1} L_h U^{k+1} + \mathcal{I}_h\phi'_+(U^{k+1}) + \mathcal{I}_h\phi'_-(U^k)] = 0. \tag{34}$$

To find this solution, we set $U_0^{k+1} = U^k$ and look for vectors U_{i+1}^{k+1} satisfying $B(U_{i+1}^{k+1}) = 0$, where

$$B(U_{i+1}^{k+1}) := U_{i+1}^{k+1} - U^k + \tau_k M_h^{-1} L_h^M(U_i^{k+1})[M_h^{-1} L_h U_{i+1}^{k+1} + \mathcal{I}_h\phi'_+(U_{i+1}^{k+1}) + \mathcal{I}_h\phi'_-(U^k)], \tag{35}$$

and iterate this procedure to identify a fixed point. We solve the nonlinear problem $B(U_{i+1}^{k+1}) = 0$ by Newton's method. So we set $U_{i+1,0}^{k+1} = U_i^{k+1}$ and determine $U_{i+1,j+1}^{k+1}$ by

$$U_{i+1,j+1}^{k+1} = U_{i+1,j}^{k+1} + \alpha_j Y^j,$$

where the direction Y^j is given by $DB(U^{k+1}_{i+1,j})^{-1}B(U^{k+1}_{i+1,j})$. The stepsize α_j is chosen according to Armijo's rule. Thus in each step of Newton's method, we have to solve a linear system involving the sparse matrix $DB(U^{k+1}_{i+1,j})$. For this purpose we apply a preconditioned BiCGstab [43] algorithm.

Hence, we obtain a sequence U^{k+1}_{i+1} of approximate solutions. If $\|U^{k+1}_{i+1} - U^{k+1}_i\|$ becomes sufficiently small, we set $U^{k+1} = U^{k+1}_{i+1}$ and continue with the next timestep. Usually, only four to ten steps are required to get below an error tolerance of 10^{-10}.

The solution calculated by this scheme satisfies a discrete version of the energy estimate. Thus we are able to bound the discrete energy $\int_\Omega |\nabla U(T)|^2 + \mathcal{I}_h\phi(U(T))$ at time T by the discrete energy at time 0. Similarly, we can bound the discrete entropy $\int_\Omega G_\sigma(U(T))$ at time T by the discrete entropy at time 0 with the help of a discrete version of the entropy estimate. Thus, using the strategies known from the continuous setting, non-negativity of discrete solutions follows in a natural way. Furthermore, these estimates can be used to proof convergence of the scheme (see [30–32]).

4.2. Newtonian liquid films on heterogeneous substrates

So far, we have always assumed the interface potential $\phi = \phi(u)$ not to be explicitly dependent on the spatial variable x. If we consider heterogeneous surfaces, this no longer holds true. On chemically heterogeneous surfaces, an interface potential can in principle be derived in a similar way as in the homogeneous case—by integrating over all of the corresponding pair potentials, thus leading to a potential $\phi(u, x)$ continuous in x. On a sample substrate consisting of two materials A and B separated by the boundary line at $\{x = 0\}$, the interface potential tends to the homogeneous potential $\phi_A(u)$ respectively $\phi_B(u)$ for $x \to \pm\infty$. In the thin-film approximation—where we assume that the lateral distances are much greater than the film thickness—the interface potential is in leading order discontinuous: $\phi = \phi_A$ on part A and $\phi = \phi_B$ on part B of the substrate (see [21]).

In this chapter we will present numerical results for such potentials piecewise constant in x and we will cite convergence and non-negativity results.

Our algorithm is inspired by the scheme presented in the previous section (for details, see [3]). As already mentioned above, the key idea of this scheme is to make entropy and energy estimates available also in the discrete setting. Endowed with these estimates we are able to obtain results on non-negativity and convergence of discrete solutions. The approximation properties of discrete solutions to this scheme are summarized in the following theorem.

Theorem 4.1. *Let us assume that for a polygonally bounded substrate* $\Omega = \Omega_A \cup \Omega_B$ *the potential* $\phi(u, x)$ *is given by*

$$\phi(u, x) = \begin{cases} \phi_A(u) & \text{if } x \in \Omega_A \\ \phi_B(u) & \text{if } x \in \Omega_B. \end{cases}$$

In addition, let $\phi(u, x)$ *be bounded from below by a constant* C *and let* $\phi_{,u}(u, x) := \frac{\partial}{\partial u}\phi(u, x) \in L^\infty(\mathbb{R} \times \Omega)$.

Then there exists a pair of functions (u, p), $u \in L^2(0, T; C^\beta(\Omega))$, $0 < \beta < 1$, *and* $p \in L^2(\Omega_T)$ *such that*

$$\int_0^T \int_\Omega (u - u_0)\partial_t\psi = \int\int_{[u>0]} m(u)\nabla p\nabla\psi \tag{36}$$

for all $\psi \in C^1(\Omega_T)$ *with* $\psi(\cdot, T) = 0$ *and*

$$\int_0^T \int_\Omega (p - \phi_{,u}(u, \cdot))\theta = \int_0^T \int_\Omega \nabla u\nabla\theta \tag{37}$$

for all $\theta \in C^1(\Omega_T)$. The non-negative function u satisfies an entropy estimate, and a subsequence of discrete solutions $U_{\tau,h}$, $P_{\tau,h}$ converges to u, p as the discretization parameters τ and h tend to zero.

Remark. For a mathematically detailed statement and for the proof of this theorem, we refer to [3].

Note that the theorem does not apply to the effective interface potential

$$\phi(u,x) = \begin{cases} -a_2 u^{-2} + a_8 u^{-8} & \text{for } x \in \Omega_A \\ -b_2 u^{-2} + b_8 u^{-8} & \text{for } x \in \Omega_B. \end{cases} \tag{38}$$

Nevertheless, if we replace ϕ by a potential $\phi_\varepsilon(u,x)$ which is linearized for values of u below a positive threshold parameter ε, then theorem 4.1 applies and a solution to the modified problem exists. For the sake of numerical stability (excluding the possibility of division by zero), this replacement is necessary in the algorithm, anyway. If the solution to the modified problem remains bounded from below by ε for all times, then it obviously solves the original problem, too.

In one space dimension, we are able to prove strict positivity, if initial data are strictly positive and the potential is of the form (38). In detail, the following theorem holds.

Theorem 4.2. *Assume that $N = 1$, ϕ satisfies (38), and that initial data are strictly positive. Then there exists a pair of functions (u, p), $u \in C^{1/2,1/8}(\Omega_T)$ and $p \in L^2(\Omega_T)$, such that*

$$\int_{\Omega_T} (u - u_0)\partial_t \psi = \int_{\Omega_T} m(u)\partial_x p \partial_x \psi \tag{39}$$

for all $\psi \in C^1(\Omega_T)$ such that $\psi(\cdot, T) = 0$ and

$$\int_{\Omega_T} (p - \phi_{,u}(u,\cdot))\theta = \int_{\Omega_T} \partial_x u \partial_x \theta \tag{40}$$

for all $\theta \in C^1(\Omega_T)$.

Moreover, there is a positive real number γ such that $u \geqslant \gamma$ on Ω_T, and the discrete solutions $U_{\tau,h}$, $P_{\tau,h}$ converge to u, p for $\tau, h \to 0$ in the following sense.

- *$U_{\tau,h} \to u$ uniformly in Ω_T.*
- *$P_{\tau,h} \rightharpoonup p$ weakly in $L^2(\Omega_T)$.*

For the details we refer once more to [3].

A numerical example is presented in figure 4. Here, the potential is of the form (38) with $b_2 = 0$. Ω_B is 'O' shaped, $\Omega_A = \Omega \setminus \Omega_B$. Apparently, the fluid tends to concentrate on the hydrophilic part Ω_B. For large t, the film morphology mimics the geometry of the substrate.

4.3. Non-Newtonian flow on homogeneous substrates

It is the aim of this section to present a numerical scheme to equation (14). We will confine ourselves to the one-dimensional case $N = 1$, so we will consider the problem

$$\begin{aligned} &u_t + \partial_x \left(u^{\frac{2\alpha+1}{\alpha}} |u_{xxx}|^{\frac{1-\alpha}{\alpha}} u_{xxx} \right) = 0 \qquad \text{in } \Omega \times (0,T), \\ &u(0,\cdot) = u_0 \qquad \text{in } \Omega, \\ &u_x = u_{xxx} = 0 \qquad \text{on } \partial\Omega \times (0,T). \end{aligned} \tag{41}$$

The algorithm presented uses a subtle modification of the ideas developed in [31]. For $\alpha \in (0,1)$, the main question is how to discretize the term $u^{\frac{2\alpha+1}{\alpha}} |u_{xxx}|^{\frac{1-\alpha}{\alpha}}$ in order to preserve

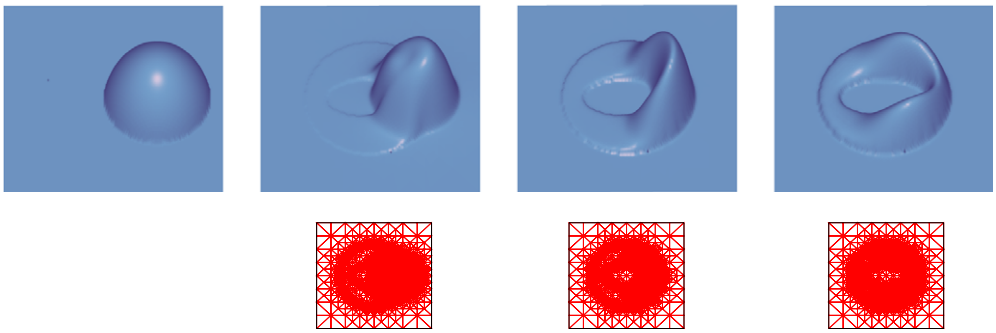

Figure 4. Thin-film flow on heterogeneous substrates: the pictures show a square of side length 2 μm at times $t = 0, 48, 845, 2377$ s. The first picture shows the initial datum: the droplet is 6 nm thick, the film surrounding the droplet is of equilibrium thickness 1.25 nm. The hydrophilic part of the substrate is 'O' shaped and corresponds to the potential $\phi(u) = \varepsilon u^{-8}$, $\varepsilon = 6.25 \times 10^{-76}$. The potential on the hydrophobic part, viscosity and surface tension are the same as in figure 3. The small pictures show the grid used in the algorithm.

non-negativity and to capture the contact line motion in a correct way. Formal considerations motivate us to split this term into a product of $u^{2+\alpha}$ and of $u^{\frac{1-\alpha^2}{\alpha}}|u_{xxx}|^{\frac{1-\alpha}{\alpha}}$ and to discretize the first term implicitly and the second term explicitly in time.

In detail, our numerical scheme appears as follows. Let $\Omega = [a, b] \subset \mathbb{R}$ be divided into subintervals $a = x_0 < \ldots < x_n = b$ of length h and V^h be the corresponding finite-element space of piecewise linear, continuous functions. Let furthermore the time interval $[0, T]$ be divided into K subintervals of length τ_k, $k = 0, \ldots, K-1$. Let U^0 be the projection of the initial value u_0 on V^h.

In the $(k+1)$st timestep, the droplet profile $U^{k+1} \in V^h$ is determined by the profile in the previous timestep via the equation

$$\int_\Omega \mathcal{I}_h((U^{k+1} - U^k)\Phi) + \tau_k \int_\Omega M_\sigma(U^{k+1}) R(U^k, P^k) \partial_x P^{k+1} \partial_x \Phi = 0 \qquad (42)$$

which has to be satisfied for all $\Phi \in V^h$. Here, $\mathcal{I}_h$ denotes the nodal projection onto V^h and P^k is just the discrete Laplacian of U^k defined through

$$\int_\Omega \mathcal{I}_h(P^{k+1}\Psi) = \int_\Omega \partial_x U^{k+1} \partial_x \Psi \qquad \forall\, \Psi \in V^h. \qquad (43)$$

The discrete substitute for $u^{\frac{1-\alpha^2}{\alpha}}|u_{xxx}|^{\frac{1-\alpha}{\alpha}}$, which has to be discretized explicitly in time, is given on each element (x_i, x_{i+1}) as

$$R(U^k, P^k)|_{(x_i, x_{i+1})} = \left(\frac{U^k(x_i) + U^k(x_{i+1})}{2}\right)^{\frac{1-\alpha^2}{\alpha}} \left|\frac{P^k(x_{i+1}) - P^k(x_i)}{h}\right|^{\frac{1-\alpha}{\alpha}}. \qquad (44)$$

The implicitly discretized part $M_\sigma(U^{k+1})$ is, in analogy to the definition in the Newtonian case (30), determined by

$$M_\sigma(U^{k+1})|_{(x_i, x_{i+1})} = \left(\int_{U(x_i)}^{U(x_{i+1})} \frac{\mathrm{d}s}{\max\{\sigma, s\}^{2+\alpha}}\right)^{-1}. \qquad (45)$$

Let us present some numerical results. Initial data to the simulation presented in figure 5 are given by a rectangular droplet profile of thickness 1 touching the left boundary of the substrate. Due to the pressure singularity at the contact line, this shape is numerically critical

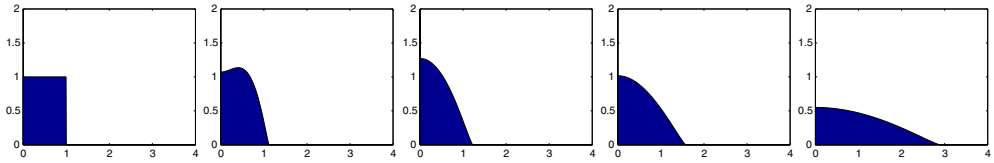

Figure 5. Spreading of a droplet for $\alpha = 1/2$. The simulation started on $\Omega = [0, 4]$ using 600 gridpoints with the following initial data: $u_0(x) = 1$ if $x \leqslant 1$ and $u_0(x) = 0$ elsewhere. We chose $\sigma = 10^{-4}$ and observed that $u \geqslant -5 \times 10^{-7}$ holds for all times. The snapshots show the droplet at times $t = 0$, 0.0001, 0.01, 1, and 1000.

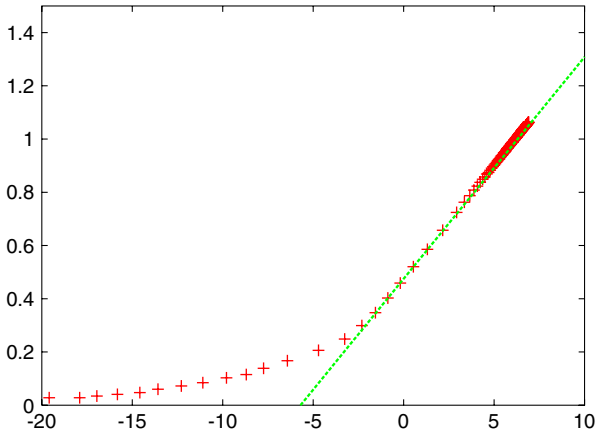

Figure 6. Propagation of the free boundary: on the x-axis we denote $\ln(t)$ and on the y-axis $\ln(x_0)$ where x_0 is the position of the free boundary in figure 5. The green line has slope $1/12$, which is the expected asymptotic propagation rate.

both with respect to non-negativity conservation and to a precise tracking of the contact line. In particular, naive approximations of the nonlinear terms would cause local negativity or non-spreading. In our scheme, however, the droplet spreads, the non-negativity properties persist and asymptotically the contact line moves according to the scaling law $x \sim t^{\frac{\alpha}{5+2\alpha}} = t^{1/12}$ which is the expected one for self-similar solutions (see section 3.3). For further numerical experiments and for the convergence analysis of this scheme, we refer to the forthcoming paper [4].

Acknowledgments

The first author has been funded by the projects Gr1693-1/1-3 within the priority programme Benetzung und Strukturbildung an Grenzflächen of Deutsche Forschungsgemeinschaft. Also the second author gratefully acknowledges the support of DFG.

References

[1] Ansini L and Giacomelli L 2004 Doubly nonlinear thin-film equation in one space dimension *Arch. Ration. Mech. Anal.* **173** 89–131

[2] Aronson D G, Betelu S I, Fontelos M A and Sanchez A 2004 Analysis of the self-similar spreading of power law fluids, submitted

[3] Becker J 2004 Numerische Simulation der Bildung fluider Strukturen auf inhomogenen Oberflächen *PhD Thesis* Universität Bonn

[4] Becker J and Grün G, Non-negativity preserving convergent schemes for the thin film equation in shear-thinning rheologies, in preparation
[5] Becker J, Grün G, Seemann R, Mantz H, Jacobs K, Mecke K R and Blossey R 2003 Complex dewetting scenarios captured by thin film models *Nat. Mater.* **2** 59–63
[6] Beretta E, Bertsch M and Dal Passo R 1995 Nonnegative solutions of a fourth order nonlinear degenerate parabolic equation *Arch. Ration. Mech. Anal.* **129** 175–200
[7] Bernis F 1996 Finite speed of propagation and continuity of the interface for thin viscous flows *Adv. Differ. Eqns* **1** 337–68
[8] Bernis F 1996 Finite speed of propagation for thin viscous flows when $2 \leqslant n < 3$ *C. R. Acad. Sci. Paris* I *Math.* **322** 1169–74
[9] Bernis F and Friedman A 1990 Higher order nonlinear degenerate parabolic equations *J. Differ. Eqns* **83** 179–206
[10] Bernis F, Peletier L A and Williams S M 1992 Source-type solutions of a fourth order nonlinear degenerate parabolic equations *Nonlinear Anal.* **18** 217–34
[11] Bertozzi A L, Grün G and Witelski T P 2001 Dewetting films: bifurcations and concentrations *Nonlinearity* **14** 1569–92
[12] Bertozzi A L and Pugh M 1996 The lubrication approximation for thin viscous films: regularity and long time behaviour of weak solutions *Commun. Pure Appl. Math.* **49** 85–123
[13] Bertsch M, Dal Passo R, Garcke H and Grün G 1998 The thin viscous flow equation in higher space dimensions *Adv. Differ. Eqns* **3** 417–40
[14] Betelu S I and Fontelos M A 2004 Capillarity driven spreading of power-law fluids *Appl. Math. Lett.* **16** at press
[15] Bird R B, Armstrong R C and Hassager O 1987 *Dynamics of Polymeric Liquids* vol 1 *Fluid Dynamics* (New York: Wiley)
[16] Carrillo J A and Toscani G 2002 Long-time asymptotics for strong solutions to the thin film equation *Commun. Math. Phys.* **225** 551–71
[17] Ciarlet Ph G 1978 *The Finite Element Method for Elliptic Problems* (Amsterdam: North-Holland)
[18] Dal Passo R, Garcke H and Grün G 1998 On a fourth order degenerate parabolic equation: global entropy estimates and qualitative behaviour of solutions *SIAM J. Math. Anal.* **29** 321–42
[19] Dal Passo R, Giacomelli L and Grün G 2001 A waiting time phenomenon for thin film equations *Ann. Scuola Norm. Sup. Pisa* **30** 437–63
[20] de Gennes P G 1985 Wetting: statistics and dynamics *Rev. Mod. Phys.* **57** 827–63
[21] Dietrich S and Rauscher M 2004 Flow over a sharp chemical step in lubrication approximation, in preparation
[22] Dussan E B and Davis S 1974 On the motion of a fluid–fluid interface along a solid surface *J. Fluid Mech.* **65** 71–95
[23] Ferreira R and Bernis F 1997 Source-type solutions to thin-film equations in higher space dimensions *Eur. J. Appl. Math.* **8** 507–24
[24] Giacomelli L and Otto F 2002 Droplet spreading: intermediate scaling law by pde methods *Commun. Pure Appl. Math.* **55** 217–54
[25] Greenspan H P 1978 On the motion of a small viscous droplet that wets a surface *J. Fluid Mech.* **84** 125–43
[26] Greenspan H P and McKay B M 1981 On the wetting of a surface by a very viscous fluid *Stud. Appl. Math.* **64** 95–112
[27] Grün G 2004 Droplet spreading under weak slippage: the waiting time phenomenon *Ann. I.H.P., Analyse Non Lineaire* **21** 255–69
[28] Grün G 2002 Droplet spreading under weak slippage: the optimal asymptotic propagation rate in the multi-dimensional case *Interfaces Free Boundaries* **4** 309–23
[29] Grün G 2003 Droplet spreading under weak slippage: a basic result on finite speed of propagation *SIAM J. Math. Anal.* **34** 992–1006
[30] Grün G 2003 On the convergence of entropy consistent schemes for lubrication type equations in multiple space dimensions *Math. Comput.* **72** 1251–79
[31] Grün G and Rumpf M 2000 Nonnegativity preserving convergent schemes for the thin film equation *Numer. Math.* **87** 113–52
[32] Grün G and Rumpf M 2001 Simulation of singularities and instabilities in thin film flow *Eur. J. Appl. Math.* **12** 293–320
[33] Hulshof J and Shishkov A 1998 The thin film equation with $2 \leqslant n < 3$: finite speed of propagation in terms of the L^1-norm *Adv. Differ. Eqns* **3** 625–42
[34] Israelachvili J 1992 *Intermolecular and Surface Forces* (New York: Academic)
[35] Jäger W and Mikelic A 2001 On the roughness-induced effective boundary conditions for an incompressible viscous flow *J. Differ. Eqns* **170** 96–122
[36] King J R 2001 Two generalizations of the thin-film equation *Math. Comput. Modelling* **34** 737–56

[37] Navier C L N H 1827 Sur les lois de l'équilibre et du mouvement des corps élastiques *Mem. Acad. R. Sci. Inst. France* **6** 369
[38] Neogi P and Miller C A 1983 Spreading kinetics of a drop on a rough solid surface *J. Colloid Interface Sci.* **92** 338–49
[39] Neto C, Jacobs K, Seemann R, Blossey R, Becker J and Grün G 2003 Correlated dewetting patterns in thin polystyrene films *J. Phys.: Condens. Matter* **15** 421–6
[40] Neto C, Jacobs K, Seemann R, Blossey R, Becker J and Grün G 2003 Satellite hole formation during dewetting: experiment and simulation *J. Phys.: Condens. Matter* **15** 3355–66
[41] Oron A, Davis S H and Bankoff S G 1997 Long-scale evolution of thin liquid films *Rev. Mod. Phys.* **69** 932–77
[42] Otto F 1998 Lubrication approximation with prescribed non-zero contact angle: an existence result *Commun. Partial Differ. Eqns* **23** 2077–164
[43] van der Vorst H A 1992 A fast and smoothly converging variant of bi–cg for the solution of nonsymmetric linear systems *SIAM J. Sci. Stat. Comput.* **13** 73–86
[44] Weidner D E and Schwartz L W 1994 Contact-line motion of shear-thinning liquids *Phys. Fluids* **6** 3535–8
[45] Winkler M 2001 Entropy solutions with constant support of a fourth order degenerate parabolic equation, submitted